UPPSALA UNIVERSITET

Independent Project at the Department of Earth Sciences
Självständigt arbete vid Institutionen för geovetenskaper
2022: 19

Large-Scale Atmospheric Drivers of Extreme Temperature Anomalies During Springtime in the Arctic

Storskaliga atmosfärsmönster som bildar extrema temperaturavvikelser under våren i Arktis

Linnea Barreng

DEPARTMENT OF EARTH SCIENCES
INSTITUTIONEN FÖR GEOVETENSKAPER

Independent Project at the Department of Earth Sciences
Självständigt arbete vid Institutionen för geovetenskaper
2022: 19

Large-Scale Atmospheric Drivers of Extreme Temperature Anomalies During Springtime in the Arctic

Storskaliga atmosfärsmönster som bildar extrema temperaturavvikelser under våren i Arktis

Linnea Barreng

Copyright © Linnea Barreng
Published at Department of Earth Sciences, Uppsala University (www.geo.uu.se),
Uppsala, 2022

Abstract

Large-scale atmospheric drivers of extreme temperature anomalies during springtime in the Arctic
Linnea Barreng

In this project warm extreme temperature events in the Arctic region during the spring months March, April and May were identified and analysed. In the analysis daily average NCEP reanalysis data from NOAA/OAR/ESRL PSL format was used. The extreme events were retrieved as the highest positive temperature anomalies from the climatological mean, and the synoptic scale plots for the 50 most extreme events were created to identify what patterns caused the extreme warming over the Polar region. By contouring the areas of statistical significance, the regions with a reoccuring pattern were identified. The results conclude that cyclonic activity over the high Arctic extending down over Greenland and northern Canada combined with anomalously high geopotential height over the north Pacific ocean, over the Arctic and towards Siberia cause the high temperatures over the pole. A weaker Polar Vortex causes pertubations in the jet stream, ridges in these Rossby waves can act as a pathway for warm and moist air from the oceanic regions which has a warming effect in the Arctic. Further analysis can be done to investigate what teleconnections these spring-time extreme events have on a global scale.

Keywords: Meteorology, Temperature extremes, Arctic, Jet stream, Rossby waves, Spring

Degree Project C in Meteorology, 1ME420, 15 credits, 2022
Supervisor: Gabriele Messori
Subject reader: Vera Melinda Gálfi
Department of Earth Sciences, Uppsala University, Villavägen 16, SE-752 36 Uppsala (www.geo.uu.se)

The whole document is available at www.diva-portal.org

Sammanfattning

Storskaliga atmosfärsmönster som bildar extrema temperaturavvikelser under våren i Arktis
Linnea Barreng

Under detta projekt har extremt varma temperaturevent i Arktisområdet under vårmånaderna Mars, April och Maj identifierats samt analyserats, genom att använda daglig medelvärdes NCEP reanalys data från NOAA/OAR/ESRL PSL i NetCDF format. De extrema händelserna identifierades genom att ta de största positiva temperaturavvikelserna från ett klimatologiskt medelvärde, storskaliga avvikelseplottar skapades för de 50 mest extrema händelserna för att kunna identifiera meteorologiska mönster som ovanligt varma Arktisdagar. De områden med mest återkommande mönsterna var statistiskt signifikanta och markerades med svarta konturer. Resultaten visar att lågtrycksaktivitet i Arktis som sträcker sig ner över Grönland samt norra Kanada kombinerat med höga geopotentialhöjdavvikelser över Stilla havet och Sibirien som sträcker sig upp mot Nordpolen orsakar ovanligt höga temperaturer i Arktis. En svag polarvirvel orsakar störningar i jetströmmen, dessa ryggar i jetströmmen kan transportera varm fuktig luft från haven mot polen vilket kan ha en värmande effekt. Vidare forskning kan utföras för att identifiera de exakta kopplingarna och konsekvenserna som dessa varma extrema Arktishändelser har globalt.

Nyckelord: Meteorologi, Arktis, Extremväder, Jetström, Rossbyvågor, Vår

Examensarbete C i meteorologi, 1ME420, 15 hp,v2022
Handledare: Gabriele Messori
Ämnesgranskare: Vera Melinda Gálfi
Institutionen för geovetenskaper, Uppsala universitet, Villavägen 16, 752 36 Uppsala (www.geo.uu.se)

Hela publikationen finns tillgänglig på www.diva-portal.org

Contents

1. Introduction

Arctic surface temperatures increase at a higher rate than the global average due to anthropogenic warming triggering a positive feedback-loop called Arctic Amplification (AA). This Arctic sensitivity to climate change is due to several different mechanisms such as sea ice albedo feedback, radiative forcing and turbulent heat fluxes from the Arctic Ocean (Cohen et al. 2018). Surface warming in the Arctic region leads to the melting of snow, land ice and sea ice, causing lower albedo properties at the surface. The albedo indicates how much of the incoming solar radiation is reflected, with a lower albedo, a larger portion of this shortwave radiation is absorbed and in turn causes lower tropospheric warming in the Arctic. AA and the increased frequency of extreme events have teleconnections around the world, for example extremely cold Eurasian and North American winters (Messori, Woods & Caballero 2018; Wegmann et al. 2015; Cohen, Pfeiffer & Francis 2018) which can have a huge effect on human lives.

Sea-ice coverage (SIC) in the Arctic ocean has its annual minima during late summer, if the SIC is low, a larger portion of the region will be open water (Przybylak 2015). Open water areas are a great heat and moisture source during the coming cold wintertime months. A meandering jet stream allows warm moist air from the Atlantic or Pacific oceans to access the Arctic region, whilst also letting cold polar air from the Arctic flow towards the continents. Cyclones (low pressure systems), originated at lower latitudes moving north, bring warm moist air to the polar region. So anomalously high wintertime temperatures in the Arctic have been linked to low SIC, combined with perturbations in the jet stream and cyclonic behaviour (Binder et al. 2017; Landrum & Holland 2020; Riboldi et al. 2020).

Several studies have investigated the weather patterns during extremely warm and cold events during the winter- and summertime in the Arctic (Messori, Woods & Caballero 2018; Woolings, Harvey & Masato 2014). But what processes cause these events during the spring and autumn months? Will similar patterns occur during spring as during the winter, or will factors such as the increased incoming solar radiation change the large-scale drivers? This is what will be investigated during this project.

The aim is to identify the extremely high temperature anomalies in the Arctic region (latitudes north of 80°N) during the spring months between the years 1948-2021. The 50 most extreme events will be averaged and will represent how extremes in the area are usually formed. By comparing this average and previous studies with the most extreme events, conclusions can be made if the most extreme synoptic scale patterns differ for different seasons. A large amount of meteorological variables can be used to thoroughly analyse the atmospheric behaviour, but during this project only the surface air temperature, air pressure and geopotential height will be used. To get a deeper understanding of the effects extreme events such as these have on a global level and what consequences they can have on humans', further investigations over a larger timescale and area can be done, but this will not be performed during this project.

2. Background

2.1 The Arctic climate

Because of its location at the pole of our planet, the Arctic differs in its climatological characteristics compared to the rest of the globe. Due to the Earth's tilt and movement around the sun, the poles experience polar summers and winters, where there is minimum incoming solar radiation during the winter and 24-hour sun shine during the peak of the summer months.

The two polar regions Arctic and Antarctic differ from each other due to their differences in location, the Antarctic being land surrounded by ocean whereas the Arctic is the opposite. The high latitude area consisting of ocean encircled by land has a central part called the Arctic ocean, which is mainly covered with ice all year round. This Arctic ocean and surrounding sea covers an area of 14 million km^2; during late winter, almost all of this area is covered by sea ice, whilst during the late summer the sea ice extent (SIE) is at an annual minimum of about 8 million km^2 (Przybylak 2015). Seen in figure 1. Due to anthropogenic warming these numbers have declined by about 31% since the beginning of the satellite era until today (Landrum & Holland 2020).

The sea ice has an important role in the Arctic climate for several reasons. Firstly, sea ice has a high albedo (0.5-0.7) in comparison to open waters (0.1). Albedo is a factor of the incoming solar radiation and the reflected outgoing radiation, which tells us how much of the solar energy is absorbed by the surface. Snow, ice and similar surfaces will have a high albedo due to the amount of reflected shortwave radiation in comparison to, for example, water or asphalt where a larger portion of the suns' energy will be absorbed. The sea ice have a greater cooling effect than open ocean. Secondly, sea ice also has an insulating effect, and will block some of the moisture and heat exchange between the ocean and atmosphere. A third attribute is that the sea ice delays the seasonal temperature cycle due to it having the properties of a thermal reservoir (Przybylak 2015).

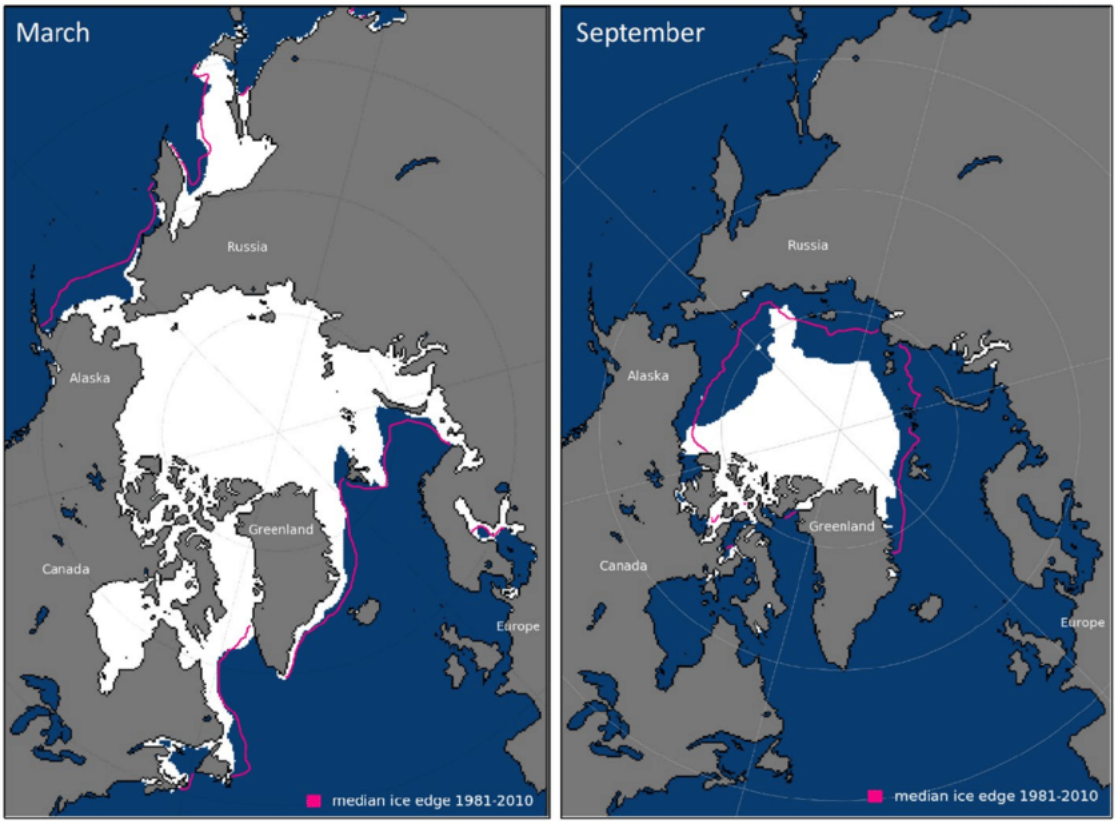

Figure 1. The figure shows the average sea ice extent in the Arctic basin for the months of March and September in 2018. The magenta line represents the median SIE for the time period 1981-2010. Image courtesy of the National Snow and Ice Data Center, University of Colorado Boulder (Fetterer et al., 2017).

2.2 Temperature extreme events

To create a better understanding of the climate and weather it is important to identify and analyse so called "extreme events". Specifically temperature extremes are valuable to map due to the consequences they have in a time where global warming is very relevent. In this project, the most extreme event was defined as the largest positive temperature deviation from the climatological mean, in other words when the 2 meter surface air temperature had the highest positive anomaly.

Events such as these in the Arctic can be linked to weather-patterns in other areas on the planet. Different studies suggest a link between heat waves in the Arctic and colder temperatures in regions such as Eurasia and North America, known as "warm Arctic cold continent" (Wegmann et al. 2015; Messori, Woods & Caballero 2018; Riboldi et al. 2020), caused by changes in Rossby wave amplitude and phase speed. A more detailed explanation of the effect of Rossby waves on the jet stream can be found in section 2.3. When the temperature difference between the two areas is large, the jet stream is strong and does not meander greatly. When the Arctic is warmer, however, the temperature gradient is weaker, thus leading to an intensification in the Rossby wave activity.

Several studies, (Riboldi et al. 2020; Clark & Lee 2019 etc) , discuss that sea ice

decline can be the cause for changes in the polar vortex, leading to an interference with Rossby waves and cold air being pushed towards the lower latitudes. This theory links Arctic Amplification with the cold continent extremes. AA is the positive feedback loop caused by several different atmospheric and oceanic mechanisms such as the Arctic surface albedo (Cohen et al. 2018). The melting of ice triggers more of the incoming solar radiation to be absorbed by the surface and as a consequence the surface gets warmer and melts. Riboldi et al. (2020) concludes that Arctic Amplification is not the cause for reduction of Rossby waves phase speed. However events with reduced phase speed do coincide with temperature extremes and atmospheric blocking (Riboldi et al. 2020).

2.3 Synoptic-scale Meteorological Patterns

When analysing a meteorological event, a lot of understanding can be gained by looking at the sea level pressure. The air pressure indicates how the air in the atmosphere is moving. Low pressure systems, also known as cyclones, indicate rising air seen as clouds and precipitation. Cold and warm air circulate counter clockwise around these cyclones in the northern hemisphere (McIlveen & McIlveen 2010). Cyclones occur in the high latitudes all year round but certain places experience semi-permanent low pressure systems, for example the Icelandic low which can be found between Iceland and southern Greenland. This system causes strong winds over the North Atlantic Ocean during the winter-time due to the differences in sea and continent temperatures (Przybylak 2015). During the summer this North Atlantic Oscillation (NAO) weakens because of the rise in temperature over the continents, thus the temperature gradient is weaker; the Icelandic low then splits into several cells .

High pressure systems, known as anticyclones are important to observe in the Arctic region due to their cooling properties. The anticyclones are larger than cyclones, rotate in a clockwise direction, in the Northern hemisphere, and consist of converging air at the top, divergent air close to the surface (McIlveen & McIlveen 2010). Some characteristics that these systems have during wintertime in the northern hemisphere are cold temperatures and clear skies. The polar anticyclones move towards the equator in a eastward direction, which brings the cold polar air towards the continents. A semi-permanent high pressure system called the Siberian high is situated in northeastern Russia during the winter and consists of cold polar air (Przybylak 2015). When this high pressure system migrates either west towards Europe or east towards northern North America, the mentioned areas can experience cold weather. Anticyclones will then lead to colder temperatures for the Arctic region, so when experiencing extremely high temperature anomalies in the Arctic one can expect to see cyclonic activity in the polar region.

The lowest part of the atmosphere called the troposphere ends at a certain air pressure level. This edge of the troposphere is called the tropopause and its altitude varies around 15km (McIlveen & McIlveen 2010). Polar regions consist of cold dense air causing the tropopause to be located at lower altitudes compared to the equator which consists of warm, rising air. In the upper troposphere over the mid-latitudes a stream of air flowing at very high speeds is moving west to east around the globe

called the Polar jet stream (McIlveen & McIlveen 2010). It is formed due to the strong temperature differences between the polar and the subtropical air masses, the polar air is colder and therefore more dense than the warmer air from the equator.

This upper tropospheric circulation can also be described as the Polar Vortex, where if the temperature gradient between northern and southern latitudes is great the Polar Vortex is strong and stable; when the temperature gradient is low the Polar Vortex is weak so the jet stream meanders. Extreme events are more likely during a weak Polar Vortex (Przybylak 2015). This meandering looks like vertical waves along the jet stream and are called Rossby waves. Ridges in the Rossby waves are when the jet stream curve northward, allowing southern warm air to flow north, while troughs are the opposite, when the jet stream curves south so polar air moves south.

To get an indication of the jet streams path, the geopotential height can be used. Geopotential height approximates the height from the mean sea level surface for a certain air pressure level, in this study the air pressure of 500hPa is used. So when only mapping the 500 hPa geopotential height spatially for a certain time, areas with lower values will represent colder air masses. The areas with warmer air will have risen so the air pressure of 500 hPa will be at a higher altitude than the colder air mass (McIlveen & McIlveen 2010).

2.4 Previous studies and hypothesis

In Messori, Woods & Caballero (2018) they investigate the atmospheric drivers that cause both warm and cold extreme temperature anomalies in the Arctic during the winter months November-March. The cold extremes were caused by a strong Polar vortex, blocking moisture intrusions that would have hindered the rapid radiative cooling (Messori, Woods & Caballero 2018). The study concludes that the positive extremes coincide with low sea level pressure anomalies over the Arctic basin and high anomalies over Eurasia. Moisture intrusions into the high latitudes from the Atlantic play an important role in the high temperatures, Messori et al. (2018) hypothesises that these moisture intrusions reach the polar region through several different cyclones. The cyclonic systems are frequent in the north Atlantic, but do not penetrate the highest latitudes, hence the polar cyclones are most likely locally formed. The two areas that experience the most significant cyclones during the warm extremes are the north Atlantic east of Greenland and the high Arctic, this can also be seen in Wegmann et al. (2015). Messori et al. (2018) also investigates the Warm Arctic Cold Eurasia phenomena and concludes that warm Arctic temperature anomalies are systematically associated with negative Eurasian temperature anomalies within a 10 day period.

Tropically Excited Arctic warming Mechanism (TEAM) could be a reason for the warm Arctic- cold continent phenomena, which is presented in Clark & Lee (2019). During the past decades the sea surface temperature gradient between the east and west tropical Pacific Ocean has increased, these conditions have La Niña like behaviour and can be linked to ENSO. For definition of La Niña and ENSO see NOAA (2021). TEAM indicates that tropical convection seen in La Niña conditions causes the Rossby wave to meander which leads to heat and moisture flux from the Pacific into the Arctic region. The perturbations in the Rossby waves weakens the polar

vortex which can lead to extreme cold temperatures over the mid-latitude continents (Clark & Lee 2019).

In December 2015 an extreme warm event took place in the Arctic. Moore (2016) concludes that the extreme warm event occurred due to perturbations of the polar vortex. These perturbations led to the jet stream flowing pole-wards and bringing warm and moist air towards the Arctic, which agrees with Riboldi et al. (2020) conclusions. In the lower parts of the troposphere high levels of water vapour likely caused down-welling longwave radiation onto the surface which increased the temperature. Moore (2016) states that the sea ice coverage (SIC) reduction was the largest reduction between two following days in 15 years. And discusses that due to it being a one-day SIC reduction, it should be analysed with caution. The reduction could be because a consequence of issues with the measurements of SIC when there has been precipitation, due to water on ice can falsely identify as areas of open water.

Binder et al. (2017) also identifies the causes for the extremely high temperatures in December 2015. They conclude that three different warm air masses were transported to the pole through an intense low-level jet that was formed between a series of North Atlantic cyclones and a quasi-stationary anticyclone over Scandinavia. These three air masses came from warm subtropical low-level air, low-level cold polar air heated by intense surface heat fluxes. And lastly upper tropospheric, cold mid latitude air, descended from the anticyclone over Scandinavia and was adiabatically heated. Binder et al. (2017) also reminds the reader that an extreme event such as this was not only caused by the unusual processes that coincide, but also by a long-term warming trend on the globe, especially in the polar regions.

So to conclude, synoptic scale patterns that are likely present during an extreme warm event in the Arctic are:

- Low pressure systems in the high Arctic and the north Atlantic, with anticyclones over Eurasia and North America
- Moisture intrusions into the high latitudes
- Rossby wave ridges over the Pacific and Atlantic ocean to allow the warm and moist air to be transported to the Arctic

3. Method and Data

3.1 Data used

The data used for this project was NCEP reanlysis daily average data provided by the NOAA/OAR/ESRL PSL (NOAA 2022) in NetCDF format. The NCEP reanalysis data comes from an analysis/forecast system that performs data assimilation using both in situ measurement data and satellite data from 1948 to present day. Air temperature data at 2 meters above the surface was used for the part of the analysis to determine the extreme events. Apart from the temperature data, geopotential height and sea level pressure data was used when analysing the extreme events. This was daily average data between the years 1948-2021. The Arctic region was defined as the area north of latitude 80°N, this area is presented as a black contour in figure 6a). When looking at synoptic scale patterns, grid points above latitude 40°N was used.

3.2 Analysis

The data handling was divided into two parts; the first being getting the extreme events from temperature anomalies and the second part focuses on the analysis of these events.

The main part of the analysis was done in MatLab, but to easier handle the data the Cygwin package *Climate Data Operators* (CDO) was used. In CDO the leap days were removed along with all the grid points outside the area of interest. For the geopotential height data, only the 500hPa level was considered. The months March, April and May were chosen to represent the spring period. Lastly the daily means were calculated using CDO.

The surface air temperature daily mean series was smoothed using a running mean function in MatLab over 15 days. This daily mean series, also known as the climatological series was used to subtract from the actual 74- year data to get the anomaly-series. Due to the Earths' spherical shape the horizontal distances between grid points at higher latitudes were shorter. To correct this, latitude-weighting was performed.

The temperature anomaly series was smoothed over 7 days and as a result of global warming it had a positive trend. Using Matlabs detrend function the linear warming trend was removed, the anomaly temperature series for the Arctic was done. When getting the extreme events a spatial mean in the defined Arctic region was used. After the anomaly series was created the time series was rearranged from highest to lowest anomalies and the 300 highest values were selected. Reasonably, a lot of the dates were subsequent and would then technically be the same event. The extreme event was then defined to be the highest anomaly within a 21 day period. So starting from the top of the array, other values within 10 days before and after were removed. To have a sufficiently large sample size, and having a good balance between the extremeness of different events, the 50 most extreme events were extracted.

Once the extreme events were found, the two events with the highest temperature anomalies were analysed separately to investigate whether these were similar to typical extreme events. Surface air temperature, sea level pressure and 500hPa geopotential height for these two days is presented in the results in section 4., the NCEP reanalysis data for the two days were plotted using a package called m_map in Matlab. The anomaly spatial field is also plotted for the two most extreme events.

To get an understanding of how extreme temperature events were formed, synoptic scale maps were created for the three variables. In these synoptic charts all calculations were done for each grid point above 40°N. For each variable a mean was taken for all 50 extreme day anomalies. 10 and 5 days before and after each extreme event were extracted, categorised together, and a time mean was calculated for each. By plotting anomaly charts days before and after the event, one can create an understanding for how the high temperatures are formed.

3.3 Statistical significance

To be able to analyse what characteristics are frequent for extreme temperature events a statistical test was done, which was investigating the statistical significance.

Every grid point consists of 50 extreme days with a mean value for the 50 days. A certain point is statistically significant if 2/3 of all the anomalies have the same sign, so either negative or positive. The sign also has to be the same as the mean anomaly value of that point.

This was done for the entire 40°N-90°N area. The significant area is shown on the anomaly plots as black contours. Each plot represents a certain amount of days before or after the extreme event, with the extreme day to the right. The contours then show what activity is frequent for high temperature anomalies.

3.4 March variability

The frequency of the extreme events are not evenly distributed over the spring months. This is due to the great variability during the month of March in comparison to April and May, which can be seen in table 1.

Table 1. The frequency of extreme events for each of the spring-time months from the 50 most extreme positive surface air temperature anomaly events.

Month	Frequency
March	34
April	12
May	4

When the climatological mean and temperature anomalies are calculated, it is important to note that the extreme events are frequent in March. Which can been seen in table A.1 in Appendix. The reason for this is the variability in temperature during March. The first spring month varies a lot in temperature from year to year so the anomalies from the mean will be larger than other months.

During this study there will not be any normalisation of this variability, so it is important to keep in mind that it is normal for extreme events to be very frequent in March in comparison to April and May where the temperature is more constant, seen in table 1. To confirm this theory the standard deviation of the anomaly was calculated in MatLab, so the standard deviation for each day in the March, April , May (MAM) data-series. In figure 2 this is seen, and it is clear that March has the greatest standard deviation of the anomaly.

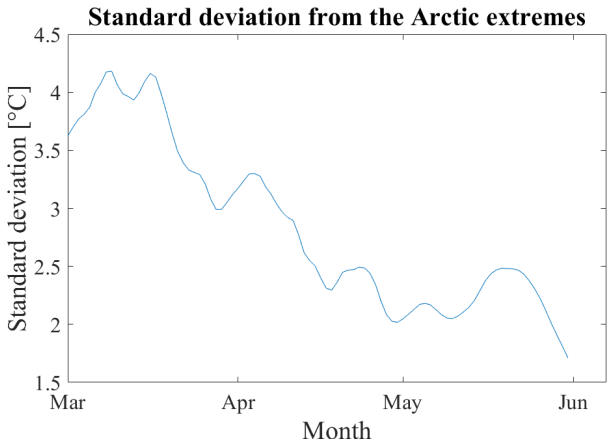

Figure 2. Standard deviation of the Arctic springtime temperature anomaly series.

4. Results

From the analysis of finding the highest positive temperature anomalies for the Arctic region during the spring months March, April and May, the 50 most extreme events were extracted as seen in table 1. To see what synoptic scale patterns these warm extreme events have, the mean anomaly for all 50 days for each grid point was calculated and can be seen in figures 3, 4 and 5. Where figure 3 is the temperature data in $^{\circ}C$, figure 4 is for the sea level pressure with unit hPa and figure 5 shows the 500hPa geopotential height in m. The black contours in the images represent the area of statistical significance.

4.1 Temperature

In figure 3 one can see that the high temperatures develop in a short amount of time. 10 days before and after the extreme event do not show clear indications of a certain specific area of significance. Whilst for the positive and negative lag 5, which is five days before and after the event, an indication of a temperature maxima can be observed. Five days before the extreme event, the area of statistical significance is extended from the north Pacific ocean to northern Scandinavia and northwest Siberia. Very cold anomalies are seen in the northern parts of North America. Similar behaviour is seen for lag 0, with the difference that the positive significant area is more centred above 70°N. For the extreme day a significant cold area has also developed in the eastern part of Russia southwards into Mongolia. At 5 and 10 days after the extreme event, these areas becoming warmer and the temperatures becomes closer to the mean. There is no significantly cold anomalies after the extreme event, and the positive anomaly is weaker but still has a significant area.

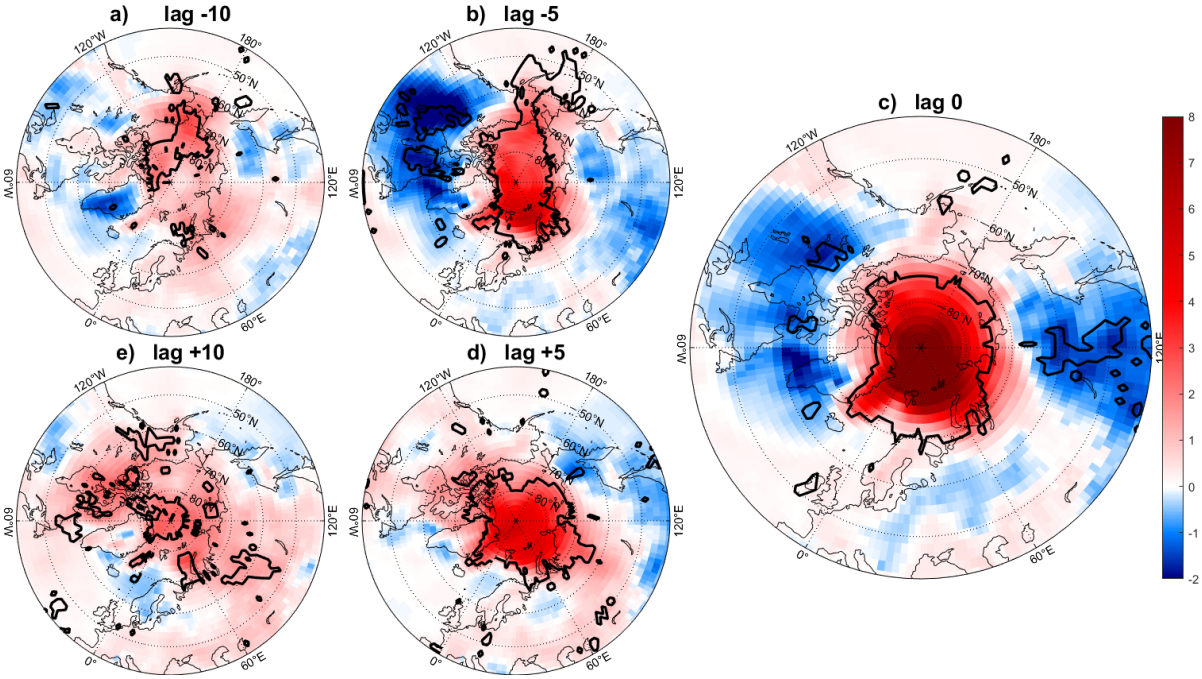

Figure 3. 2 meter air temperature anomalies from the climatological time series, in unit °C, is shown in the panels. The anomalies are mean values at each grid point for the 50 most extreme events presented in table 1. The atmospheric movement seen in lags -10 days (a), -5 days (b), 0 days (c), +5 days (d) and +10 days (e). The black contours show the areas of statistical significance.

4.2 Sea level pressure

Similar to the temperature data, 10 days after the extreme event do not show much of a specific activity. However, 10 days before the event, seen in figure 4a there is significant cyclonic activity in the northern parts of the Pacific. Over Siberia and Russia there are high pressure anomalies, similar anticyclonic activity can be observed in the northwestern parts of North America both at 10 and especially at 5 days days before the extreme event. A large low pressure system is starting to form over Iceland at lag -5. This cyclonic activity gets stronger and peaks for the extreme day, in figure 4c, with low pressures below 5 hPa of the climatological mean. At the same time, almost the entire Russia is experiencing high pressure anomalies, over Siberia there is statistically significant areas that are above 5 hPa. Blocking activity is also occurring in the Atlantic ocean west of Ireland and over Ireland.

The anomalies decrease towards the climatological mean quickly after the extreme day. Only five days after the significant areas are quite small and sparse. Ten days after there is only reoccurring low pressures in the Barents sea toward the continent. Interesting to note here is that high pressure anomalies are covering the Arctic ocean.

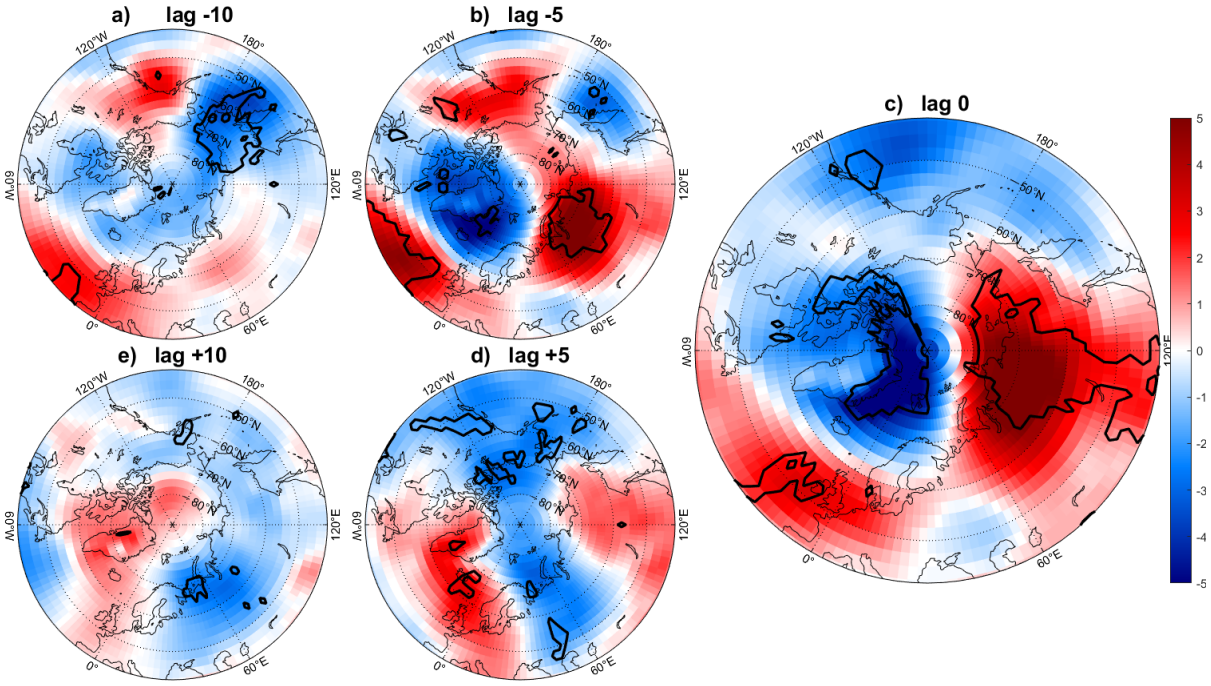

Figure 4. Sea level pressure anomalies from the climatological time series, in unit hPa, is shown in the panels. The anomalies are mean values at each grid point for the 50 most extreme events presented in table 1. The atmospheric movement seen in lags -10 days (a), -5 days (b), 0 days (c), +5 days (d) and +10 days (e). The black contours show the areas of statistical significance.

4.3 Geopotential height

The mean for the 50 most extreme days 500 hPa geopotential height anomalies for five different time steps are presented in figure 5. Ten days before the event some statistically significant negative anomalies are identified and contoured in figure 5b over both the north Atlantic and Pacific oceans. These anomalies grow stronger the coming five days and also cover eastern and central parts of North America. In between these lower anomalies an area of higher geopotential heights develops. For the extreme day seen in figure 5c the ridge has become stronger and more centred over the pole, extending towards Russias northern parts. The trough is surrounding the higher anomalies and has its most significant areas in North America.

A change is seen the days after the extreme events in figures 5d and 5e. A common area for high anomalies is the Kara seas and the land just south of Kara, while negative anomalies are again strong in the northern parts of the Pacific. This area stays negative for lag 10 as well another common area is northern Scandinavia, and higher areas are mainly present in northern parts of Canada.

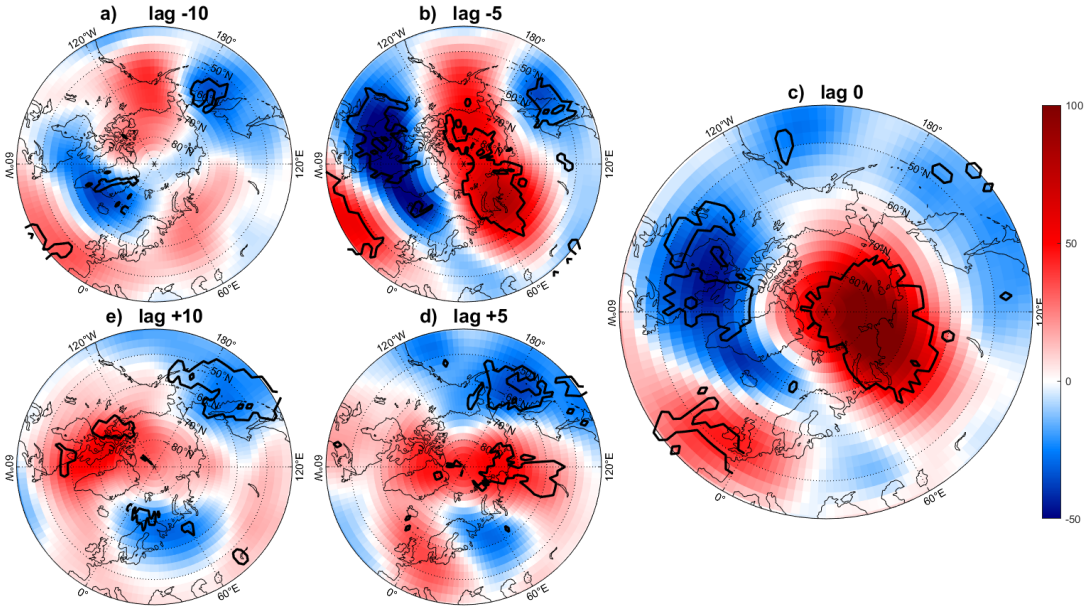

Figure 5. 500hPa geopotential height anomalies from the climatological time series, in unit meters, is shown in the panels. The anomalies are mean values at each grid point for the 50 most extreme events presented in table 1. The atmospheric movement seen in lags -10 days (a), -5 days (b), 0 days (c), +5 days (d) and +10 days (e). The black contours show the areas of statistical significance.

4.4 Two most extreme events

The two most extreme events, which are the days with highest temperature anomalies, are displayed in table 2. To see if these extremes differ or follow a similar pattern as other extreme temperature events in the Arctic during springtime, the three variables for the two days are shown in figure 6 and their anomalies displayed in figure 7.

Table 2. The two days with the highest area-averaged temperature anomalies in °C from the climatological mean.

Date	Temperature anomaly [°C]
1997-03-09	14.60
1976-03-25	12.10

The most extreme days has a 2.5 °C higher temperature anomaly than the second most extreme day, a large difference such as this indicates different atmospheric behaviour. For both events figures 6a) and d) clearly show that the oceanic regions are a great heat source. Both events experienced cyclonic activity in the Arctic region, extreme day two however had a greater negative anomaly for the day, which can be seen in panels 7b) and e). When plotting the geopotential height an indication of the jet streams behaviour can be observed, this is clear in figures 6c) and f). The cold polar air masses and the warmer southern air is divided by a yellow meandering line which can be viewed as the jet streams path.

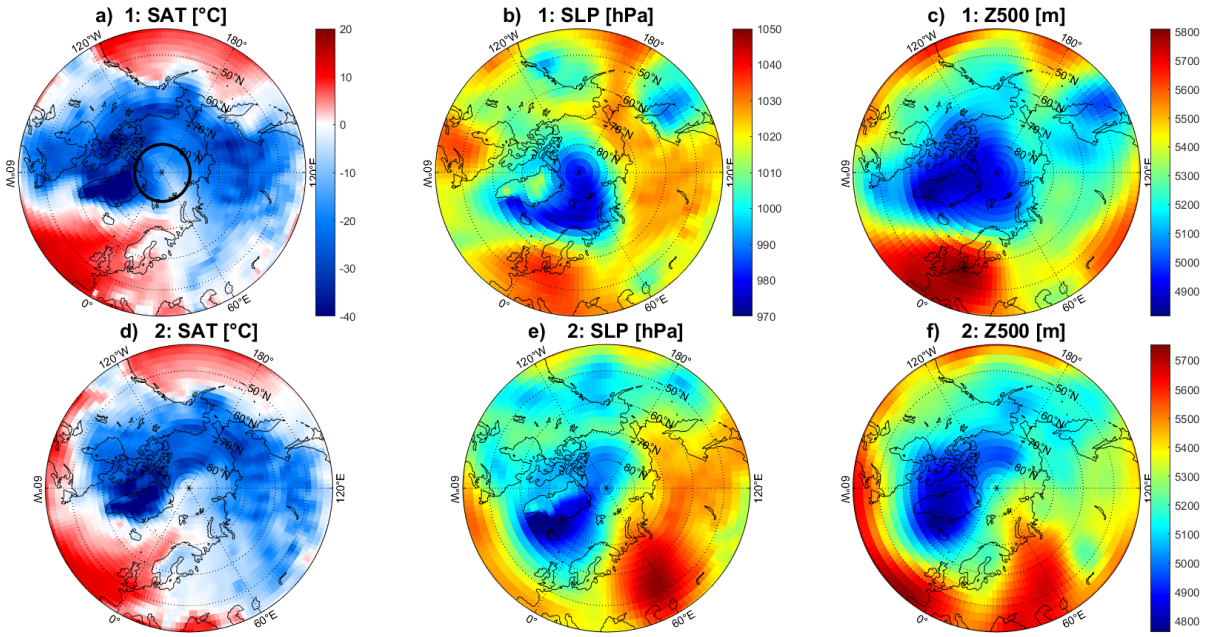

Figure 6. NCEP reanalysis data plotted at each grid point, the panels represent daily means for the most extreme events. The first extreme day 1997-03-09 in panels a)-c), and the second extreme day 1976-03-25 shown in panels d)-f). 2 meter surface air temperature in a) and d), sea level pressure in b) and e), 500 hPa geopotential height in c) and f). The contoured area in a) shows the defined Arctic region.

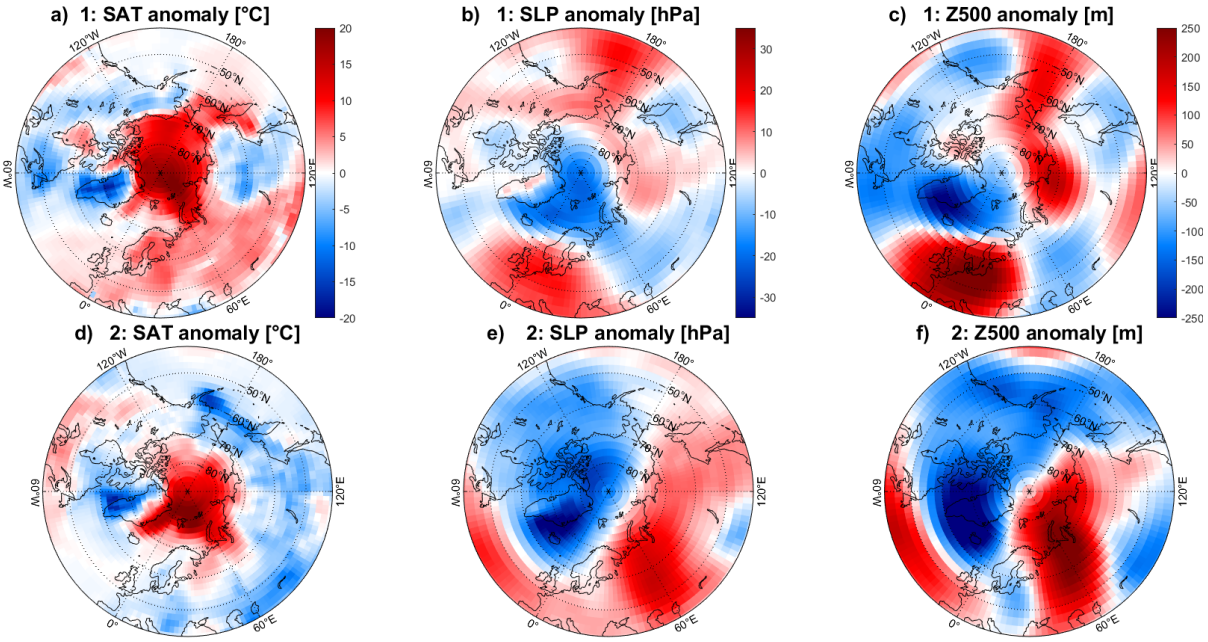

Figure 7. Anomaly data from the climatological mean plotted at each grid point, the panels represent the anomalies for the most extreme events. The first extreme day 1997-03-09 in panels a)-c), and the second extreme day 1976-03-25 shown in panels d)-f). 2 meter surface air temperature in a) and d), sea level pressure in b) and e), 500 hPa geopotential height in c) and f).

5. Discussion

5.1 Synoptic drivers

The synoptic-scale drivers seen in figures 4 and 5 contributed to the extreme temperature anomalies. The contoured, statistically significant areas show certain atmospheric patterns that are common during the extreme events.

When looking at the figures, lag -5 (figures 3b, 4b and 5b) shows clear indications of an upcoming extreme. For the temperature and geopotential height one can see warm air mass that covers the northern Pacific ocean, past the pole and down over the Kara sea onto midnorth Russia. This geopotential height is mainly significant over a large area north and south of the Kara seas. Which can mean one of three things; either 5 days before an event warm air from the Pacific and mid Russia is pushed northward to the pole, or the air has transported from either the Pacific or Russia to the Arctic. This transport of the warm air was likely due to ridges in the Rossby waves over the Pacific and/or over Siberia which links to the hypothesis presented in 2.4. Air masses that originate from the Pacific likely contain a lot of moisture which upon arrival at the Arctic can cause cloud formation. Cloud coverage over a cold Arctic can act as a blanket and hinder radiative cooling.

For the sea level pressure there is both statistically reoccurring cyclonic and anticyclonic activity that starts forming at lag -5. For the extreme event there are anomalous lows over the Arctic towards the Atlantic ocean, over Greenland and stretching to northern Canada which follows the hypothesis. These low pressure systems can cause strong winds toward the pole bringing warm air to the Arctic region. On the right side of plot 4c) high pressure anomalies are reoccurring, the high pressure systems in the northern latitudes during winter months usually cause cold temperatures due to the stable conditions. These stable conditions could potentially also be a factor causing the warmer temperatures over the Arctic due to their blocking features. The north Atlantic cyclones are forced to travel northwards from Scandinavia due to the anticyclonic behaviour over Siberia, bringing warm moist air into the northern latitudes leading to an increase in temperature.

5.2 Extreme event comparisons with mean extreme anomalies

In table 2 the two days with the highest temperature anomalies are presented, with their temperature, air pressure, and geopotential height day averaged spatial field shown in figure 6. In figure 7 the anomalies from the climatological mean is seen for the three variables. By looking at 6a) and 6d) it is important to observe the temperature differences between the oceans and continents. The month of March could be seen as a final winter month at times and has similar characteristics apart from the difference in incoming solar energy. So it would be fair to say that the Atlantic and the Pacific oceans are two big big heat sources in comparison to the much colder North American, Greenland and Asian Russian continental areas.

Therefore a ridge in the Rossby waves or jet stream over the Atlantic and/or Pacific will bring good conditions for a warm Arctic event. For extreme day one a ridge is located over the Pacific ocean bringing warm air towards the higher latitudes, another ridge can be observed over the eastern Atlantic and European area. Ridges over

both the oceanic regions allow good conditions for high temperature anomalies in the Arctic. For extreme day two a similar, sharper ridge is pushing warm air over Eurasia towards the Kara sea, the heat source was likely only the Atlantic ocean in comparison to extreme day one where the warm air has its origin from both the Pacific and Atlantic oceans. Previous studies (Messori, Woods & Caballero 2018) conclude that the the Atlantic is the most common source of warm moist air.

The sea level pressure maps in figures 6b) and 6e) show cyclonic activity over the Norwegian sea. Which indicates that a lot of air circulation covering this heat source extends beyond the 80°N latitude. As previously discussed the extreme events have reoccurring high pressure systems over Russia, this was not the case for extreme day one. In the SLP plots for this event anomalously low pressure are covering the Eurasian area, which could be a cause for the warm temperatures.

These patterns differ from the drivers seen in figures 4 and 5 which is expected because these events have caused a lot warmer temperatures than the rest of the 50 day events seen in table 1. To get a better understanding of why extreme day one was such a great extreme event a more thorough analysis should be done. It is likely that February and March during 1997 experienced anomalously high temperatures in more places than the Arctic. For example very high temperatures in Europe, combined with the meandering jet stream and lower SIC in the Arctic as a consequence of a warm period can have caused this very extreme event.

5.3 Comparison to previous studies

From known processes and previous studies a short hypothesis was made in section 2.4 when supposing that the springtime events would act similarly to wintertime extremes. The 50 extreme event anomaly temperature plots seen in figure 3 look very similar to the figures seen in Messori, Woods & Caballero (2018). Five days before the extreme event warm temperatures are stretched from the Pacific over the pole to the Atlantic, and at the extreme day this area has reduced and is mainly only in the high Arctic with greater anomalies. Looking at the air pressure both studies have similar cyclone and anticyclone positions. For the extreme day strong anticyclones have developed to the west of the Arctic centre, covering the Greenland and northern Canada, ending over Iceland. And an anticyclone over Eurasia with a thin connection towards central Europe and west or Ireland, almost identical patterns are seen in Messori, Woods & Caballero (2018).

The same goes for the geopotential height. These characteristics follow the hypothesis for the positions of high and low pressure systems. As mentioned previously, figure 5b) show a ridge in the jet stream that transports warm air from the oceans towards the pole. This could be linked to TEAM behaviour (Clark & Lee 2019).

5.4 Areas to improve and future research

With a system so complex as the Earth's atmosphere it is difficult to create a complete understanding of all processes that cause extreme events. To get a clearer picture of the patterns more variables can be used, previous studies (Messori, Woods & Caballero 2018; Wegmann et al. 2015) have studied the moisture intrusions into

and from the Arctic. It would be interesting to see if the warm air masses that were transported from the Atlantic and Pacific also had high moisture anomalies.

To see if the spring time extreme warm events were due to TEAM one could have done an analysis of the tropical Pacific Ocean. Through air and moisture backwards trajectories conclusions can be made if the warm air masses were a result of e.g. tropical convection. By looking at ENSO-index time series data, it would be helpful to see if the 50 extreme events found in this project took place during strong La Niña or El Niño conditions.

To further enhance the understanding of springtime extreme Arctic events one could also analyse the cold extremes. The springtime events in this study act similarly to warm wintertime events seen in the previous studies (Messori, Woods & Caballero 2018; Moore 2016; Binder et al. 2017), this could be because the majority of the events took place in March, in some of the studies March is regarded as a winter month. By normalising the anomaly values by the long-term daily standard deviation in the analysis, April and May would probably have had more events. Alternatively one could retrieve the extremes for each month individually to compare their synoptic patterns. There could then be a difference in the atmospheres behaviour because the temperature gradient between ocean an continent would likely be smaller.

An extension of the research is to do a similar analysis for the autumn months September, October and November. It would then be interesting to see if the atmospheric patterns would be similar to the summer season, just as the spring months in this study had similar patterns to the winter season.

To broaden the understanding of teleconnections from extremely high temperature events in the Arctic, a continue of this work can be done. By creating similar positive and negative anomalies for data over the entire Earth, one can find extremes that take place a certain amount of time after an Arctic extreme. By either using known links or maybe Lagrangian backwards trajectory methods, such as the LAGRANTO tool (Sprenger & Wernli 2015), to investigate if there are any links between the Arctic and global extremes.

6. Conclusion

Using daily average NCEP reanalysis surface air temperature data, the 50 biggest positive anomalies were identified as extreme events. The defined Arctic region was north of latitude 80°N, and the analysis was done for the spring months for the years 1948-2021. Events such as these can be linked to cold extremes over Eurasia and North America which is described by the phenomena "Warm Arctic Cold Continent" (Wegmann et al. 2015; Woollings, Harvey & Masato 2014; Cohen, Pfeiffer & Francis 2018; Messori, Woods & Caballero 2018), therefor it is important to identify warm Arctic extremes. By analysing the surface air temperature, sea level pressure and 500hPa geopotential height anomalies, synoptic scale drivers that caused the warm temperatures were identified and analysed. Low pressure systems in the high Arctic combined with perturbations in the jet stream, transporting warm moist air to the pole, are some main causes for the temperature extremes. These patterns are seen in figures 4 and 5 where low geopotential height anomalies from the Pacific and Siberia toward the Arctic are seen and could be linked to a weaker Polar Vortex causing a

meandering jet stream.

To further investigate the exact reasons for why the two most extreme events are warmer than the rest of the extremes seen in table 1, one can expand this project. By also analysing the moisture in the atmosphere over the Arctic during extreme events, and using for example a LAGRANTO tool (Sprenger & Wernli 2015) to create backwards trajectories, one can identify where the moisture intrusions come from. This combined with an investigation over large time period and analysing the sea ice coverage, one can also see what long term drivers have caused the specific extreme event.

To summarise, during this project some of the atmospheric large-scale drivers that cause extremely high temperature anomalies in the Arctic during the springtime were identified and largely coincide with previous research focusing on wintertime warm extremes.

Acknowledgements

I would like to thank all the people who helped me throughout this project, firstly my supervisor Gabriele who, with his great knowledge in the field, good advice and weekly meetings, has been a large part of this project. Without Melinda's expertise within CDO. this project would have been a lot more time consuming and not as interesting during the early stages, so my greatest thanks to you for helping me throughout this work. And lastly, but not least, a big thank you to Christoffer Hallgren for all the help with MatLab problems and opinions regarding the plots.

References

Binder, H., Boettcher, M., Grams, C.M., Joos, H., Pfahl, S. Wernli, H. 2017, "Exceptional Air Mass Transport and Dynamical Drivers of an Extreme Wintertime Arctic Warm Event", Geophysical research letters, vol. 44, no. 23, pp. 12,028-12,036.

Cohen, J., Pfeiffer, K. Francis, J.A. 2018, "Warm Arctic episodes linked with increased frequency of extreme winter weather in the United States", Nature communications, vol. 9, no. 1, pp. 869-12.

Cohen, J., Zhang, X., Francis, J., Jung, T., Kwok, R., Overland, J., . . . Smith, D. (2018). Arctic change and possible influence on mid-latitude climate and weather: A US CLIVAR white paper (No. 2018-1). (K. Uhlenbrock, Ed.). Washington, DC: U.S. CLIVAR Project Office. doi:10.5065/D6TH8KGW

Clark, J.P. Lee, S. 2019, "The Role of the Tropically Excited Arctic Warming Mechanism on the Warm Arctic Cold Continent Surface Air Temperature Trend Pattern", Geophysical research letters, vol. 46, no. 14, pp. 8490-8499.

Fetterer, F., K. Knowles, W. Meier, M. Savoie, and A. K. Windnagel, 2017, updated daily: Sea Ice Index, Version 3. Boulder, Colorado USA. NSIDC: National Snow and Ice Data Center, doi: 10.7265/N5K072F8.

Landrum, L. Holland, M.M. 2020, "Extremes become routine in an emerging new Arctic", Nature climate change, vol. 10, no. 12, pp. 1108-1115.

Messori, G., Woods, C. Caballero, R. 2018, "On the Drivers of Wintertime Temperature Extremes in the High Arctic", Journal of Climate, vol. 31, no. 4, pp. 1597-1618.

McIlveen, R. McIlveen, J.F.R. 2010, Fundamentals of weather and climate, second edn, Oxford University Press, Oxford.

Moore, G.W.K. 2016, "The December 2015 North Pole Warming Event and the Increasing Occurrence of Such Events", Scientific reports, vol. 6, no. 1, pp. 39084-39084.

NOAA/OAR/ESRL PSL, Boulder, Colorado, USA, from their Web site at https://psl.noaa.gov/data/gridded/data.ncep.reanalysis.surface.html retrieved 2022.

NOAA. What are El Niño and La Niña? National Ocean Service website, https://oceanservice.noaa.gov/facts/ninonina.html, 06/04/21.

Przybylak, R. SpringerLink (Online service) 2016;2015;, The Climate of the Arctic, 2nd 2016. edn, Springer International Publishing, Cham.

Riboldi, J., Lott, F., D'Andrea, F. Rivière, G. 2020, "On the Linkage Between Rossby Wave Phase Speed, Atmospheric Blocking, and Arctic Amplification", Geophysical research letters, vol. 47, no. 19, pp. 10021-n/a.

Sprenger, M. and Wernli, H. (2015). "The LAGRANTO Lagrangian analysis tool" - version 2.0, Geosci. Model Dev., 8, 2569–2586, doi:10.5194/gmd-8-2569-2015.

Wegmann, M., Orsolini, Y., Vázquez, M., Gimeno, L., Nieto, R., Bulygina, O., Jaiser, R., Handorf, D., Rinke, A., Dethloff, K., Sterin, A. Brönnimann, S. 2015, "Arctic

moisture source for Eurasian snow cover variations in autumn", Environmental research letters, vol. 10, no. 5, pp. 54015.

Woollings, T., Harvey, B. Masato, G. 2014, "Arctic warming, atmospheric blocking and cold European winters in CMIP5 models", Environmental research letters, vol. 9, no. 1, pp. 14002.

Appendix

A.1. Dates with corresponding surface air temperature anomalies from the climatological mean for the 50 most extreme days in the Arctic region during the spring months March, April and May.

	Date	Anomaly [°C]		Date	Anomaly [°C]
1	09-Mar-1997	14.60	26	26-Mar-1948	6.16
2	25-Mar-1976	12.09	27	21-Mar-1949	6.13
3	17-Mar-2000	11.40	28	22-Apr-1953	6.13
4	09-Mar-1972	10.98	29	29-Mar-1998	6.11
5	16-Mar-1992	10.25	30	03-Apr-2019	6.09
6	02-Apr-1995	8.88	31	24-Apr-1951	6.09
7	14-Mar-1949	8.85	32	08-Mar-1957	6.00
8	01-Apr-1950	8.33	33	03-Apr-1996	5.97
9	11-Apr-1995	8.23	34	04-May-1953	5.94
10	08-Mar-2015	8.19	35	09-Mar-1951	5.92
11	11-Apr-2006	7.90	36	20-Mar-2013	5.80
12	08-Mar-1955	7.88	37	06-Mar-2014	5.79
13	03-Mar-1962	7.74	38	22-May-1948	5.78
14	12-Mar-2016	7.61	39	20-Mar-2011	5.78
15	01-Mar-2016	7.36	40	19-May-1957	5.75
16	20-Mar-1948	7.36	41	06-Apr-2007	5.75
17	03-Mar-1997	7.29	42	29-Mar-1990	5.74
18	19-Mar-1976	7.25	43	19-Apr-2020	5.71
19	17-Mar-1951	7.12	44	25-Mar-2014	5.69
20	10-Mar-1983	7.09	45	01-Mar-1958	5.67
21	07-Mar-2002	6.86	46	27-Mar-2011	5.66
22	15-Mar-1980	6.76	47	15-Mar-1982	5.63
23	07-Mar-1967	6.61	48	08-Apr-2010	5.62
24	04-Mar-1983	6.55	49	09-Mar-2012	5.56
25	07-Apr-1959	6.25	50	15-May-1951	5.56


S. ACADEMIAE
RITAS